This document is the Accepted Manuscript version of a Published Work that appeared in final form in Industrial & Engineering Chemistry Research, copyright © American Chemical Society after peer review and technical editing by the publisher. To access the final edited and published work see https://doi.org/10.1021/ie050506w

Production and application of activated carbons made from waste tyre

R Murillo, MV Navarro, T García, JM López, MS Callén, E Aylón and AM Mastral

Instituto de Carboquímica, CSIC, M Luesma Castan 4, 50018-Zaragoza, Spain

Phone: 34 976 733977, Fax: 34 976 733318, e-mail: amastral@carbon.icb.csic.es

Abstract

Nowadays, waste tyres disposal has become a relevant environmental problem. Although pyrolysis processes seem to be a feasible alternative treatment; a proper application for generated residues is a task to be solved. In this context, the aim of this work is to valorise pyrolytic tyre char by means of the production of a useful adsorbent for air purification. An activation process with CO_2 was chosen to control the process of microporosity generation. The activation reaction and the textural properties were followed to achieve the understanding of porosity evolution. It was observed a change in the reaction rate in the first steps of the process, followed by a linear relationship between activation time and burn-off. Microporosity is generated in two main processes. At the beginning, narrow microporosity is formed, and later, a widening of the micropores is taking place. The performance of the new obtained samples for hot gas cleaning was tested by a process of Phenanthrene (Phe) adsorption in a fixed bed reactor with a process temperature of 150 ºC at low inlet concentrations. It was concluded that the porosity development, both micro and non-microporosity, increases the Phe adsorption capacity of activated carbons, likely due to a multilayer adsorption process

Keywords: A. Waste tyre; B. Activated carbon; C. Textural properties D. Phenanthrene adsorption.

1. Introduction

Waste tyres have a high content of both volatile and fixed carbon[1] which makes them an interesting solid, not only as a fuel for energy production[2] or hydrogenation processes[3], but also, in pyrolysis processes[4] to obtain different fractions of solid, liquid and gaseous products. The solid obtained by pyrolysis, around 30-40% of the rubber from tyre, could be a suitable precursor for activated carbon production.

Activated carbons are high porosity and high surface area materials manufactured by carbonization and activation of carbonaceous materials by either physical or chemical activation methods[5]. For waste tyre activation, the carbonization step is usually carried out by means of a pyrolysis step under nitrogen inert atmosphere, at temperatures ranging from 500ºC to 900ºC[6]. The activation step is carried out with steam or carbon dioxide, CO_2, at high temperatures, in order to produce a partial oxidation of the tyre char, which develops its porous system[7-10].

Several studies have been carried out in order to assess the production of activated carbons from waste tyres[10]. S_{BET} data obtained are very scattered ranging from 600 m^2/g with a stream of N_2 with 40% of steam and a 60% burn-off[10], or 640 m^2/g with 65% burn-off in a fixed bed and a stream of steam or carbon dioxide[7] to 813 m^2/g[8] or 1260 m^2/g for a 91% burn-off obtained by a thermal decomposition process surrounded by steam[10]. With respect to the applications of activated carbons, different uses have been described in the literature: (a) water purification, (b) air purification, (c) special applications such as batteries, fuel cells, nuclear power stations, and (d) others such as cigarette filters, food industry, etc[9].

Several Polycyclic Aromatic Hydrocarbons (PAHs) have proven to be carcinogens and/or mutagens; hence, their control has been extensively studied[11]. Mastral et al.[12] have shown that the process of PAHs adsorption on activated carbons is mainly occurring in the micropores, favoured by wide micropore size distributions centred in high values of pore width (around 1.2 nm). In addition, the presence of meso and macropores favours the PAH adsorption, since they are the entrance for the micropores and they increase adsorption capacity due to the formation of adsorbate multilayers[12].

The aim of this work is to valorise waste tyre by means of the production of a useful adsorbent for air purification. An activation process with CO_2 is carried out in order to improve the microporosity of the tyre char, assessing the evolution of different ranges of porosity, as well as the influence of process conditions in the porosity development. Finally, the improvement of the adsorbent performance is tested in a process of Phe removal.

2. Experimental

For CO_2 activation reactions, a tyre char obtained by carbonisation in a stainless steal fixed bed reactor was used. This solid was produced in several batch reactions of 300 g of shredded waste rubber tyre each one at 1000 ºC for 3 hours with a heating rate of 8 ºC/min and a solid yield of 40%.

To obtain the activated carbon samples, a Swept Fixed Bed reactor was used (see Figure 1). This system was described in detail elsewhere[13]. In order to perform the activation runs, a new gas line with the same configuration that allows the use of N_2, CO_2 or mixtures of both was added. The experiments were performed with a fixed sample particle diameter between 0.2-0.5 mm, a char weight of 5 g, a bed height of 10 cm (ceramic rings were used as inert) and a heating rate of 8 ºC/min. A stream of N_2 was

used to reach the reaction temperature that was changed to pure CO_2 in order to activate the tyre char once the final temperature had been achieved. Once the reaction had finished, the stream was changed again to N_2 to let the sample cool in a progressive way. The different sets of samples were carried out at 850, 900 and 950^oC and reaction times between 2 and 36 hours.

Burn-off of samples was defined as:

$$\%Burn-off = 100 \times \frac{m_{0(mf)} - m_f}{m_0 \cdot C_f} \quad [1]$$

Where:

$m_{0(mf)}$ is the moisture free initial weigh of sample, kg.

m_f is the final weigh of solid, kg

m_0 is the initial weigh of sample, kg.

C_f is the amount of fixed carbon in the char.

The samples obtained were characterised by N_2 and CO_2 adsorption at 77 and 273 K, respectively, using an ASAP 2000 (Micromeritics) apparatus. The experimental error due to sample heterogeneity was around 5% depending on the sample. The BET surface area, S_{BET}, total pore volume, V_T, at relative N_2 pressure of 0.95, and total micropore volume, W_{N2}, by using Dubinin-Radushkevich (DR) equation were obtained from experimental N_2 isotherms. The narrow micropore volume, W_{CO2}, was obtained by applying DR equation to CO_2 isotherms. Finally, data of distribution, n_{DA}, adsorption energy, E_{DA}, and average pore width, L_{DA} were also obtained by applying Dubinin-Astakov, DA equation to CO_2 isotherms.

Samples were called in the way AXXXY were A comes from activated, the XXX is related to the temperature of activation and Y is the reaction time, in hours. Thus, the sample A9002 was activated at 900^oC for 2 hours. Four activated samples of the set

obtained at 900ºC were selected with different grades of porosity development, A9002, A90010, A90020, A90036 for a broader textural study. These samples were analysed by mercury porosimetry (Quantachrome POREMASTER GT (33/60)) to obtain their intrusion and extrusion curves and pore size distribution, and by Scanning Electron Microscopy (SEM) (JEOL JSM 6400) to obtain an improved view of the samples at 80, 3000 and 25000 magnifications.

On the other side, Phe adsorption experiments were conducted on these four selected samples by using the experimental rig described in detail elsewhere[8]. To obtain the isotherm for each of the four samples selected, five breakthrough curves were obtained at 150ºC (±1ºC) and Phe concentrations between 0.0001 and 0.02 mol/m^3. Helium was used as carrier gas with a constant flow of 25 ml/min, and the bed was composed of 25 mg of adsorbent material with a 0.1-0.2 mm average particle size and 2 g of sand, with the same particle size as inert to do the bed long enough (10 cm) to assure plug flow and to avoid axial dispersion problems.

The adsorption capacities, W_{exp}, of samples at different Phe concentrations were calculated by the integration of the breakthrough curves obtained.

$$W_{\exp} = \frac{Q \cdot \left(C_0 \cdot t_t - \int_0^{t_f} C_{Phe}(t) dt \right)}{m_{CA}} \quad [2]$$

Where:

W_{exp}, is the adsorption capacity, mol Phe/kg adsorbent.

Q is the gas flow through the solid, m^3/s.

C_0 is the Phe inlet concentration, mol Phe/m^3.

$C_{Phe}(t)$ is the Phe concentration at any time, mol Phe/m^3.

m_{CA} is the weight of adsorbent, kg.

t_f is the total time, s.

3. Results and discussion

Tyre char from the pyrolysis of waste tyre shows the following chemical analyses: C 87.80%; H 0.33%; S 1.97%, moisture 0.25%, volatile matter 0.88%, fixed carbon 89.26% and ash 9.61%. Its apparent surface area was 62 m^2/g with a total pore volume of 0.34 cm^3/g and a porosity of 0.49. Therefore, its total micropore volume is very low (only around 0.03 cm^3/g) and it is basically a mesoporous material that could not be efficient for hot gas cleaning processes[12].

Influence of time and temperature on activation. The influence of activation time and temperature on the degree of burn-off achieved by the tyre char is shown in Figure 2. A linear relationship between activation time and burn-off is exhibited at the same temperature. It is also observed that when the lines are extrapolated back to the y-axis, the intercepts do not pass through the origin. These facts agree with previously published results by Cunliffe et al[7]. These authors claimed that the tyre char activation proceeded through two stages. In the first one, at low degrees of burn-off, a higher weight loss rate was taking place, likely due to the reaction of the remaining carbonized rubber. Then, a linear period of burn-off is following, where the remaining carbon black is reacting.

Concerning to the temperature influence, there is a direct correlation between temperature and reaction rate. As it was expected the higher the temperature, the higher the conversion for the same reaction time[12], see Figure 2.

Influence of reaction time on porous texture. Figures 3.a and 3.b contain the adsorption isotherms obtained for tyre char and four selected samples. It is observed that all the N_2 adsorption isotherms are type IV in IUPAC classification, produced for

solids with a mainly mesoporous structure, as other authors have previously described[14]. Comparing the isotherms, it can be observed an increase in their starting points, their slopes and their final points, probably due to the development of micro, meso and some little macroporosity, respectively. Regarding to CO_2 adsorption isotherms (Figure 3.b), there is a progressive increase in the amount adsorbed, except for the most activated one.

The textural parameters of these activated carbons, calculated from their N_2 and CO_2 adsorption isotherms, are collected in Table 1. It is observed that, as a result of the activation there is an increase in BET surface area, with a maximum observed at 68.4% burn-off, 528 m^2/g. This value is 8 times higher than the value of the char. It can be also observed that the highest variation in surface area takes place in the range from 20% to 50% of burn-off, as there are no substantial changes at the beginning of the reaction, which agree with the published data [15]. On the other hand, whilst the total and the micropore volumes linearly increase with the burn-off, the narrow micropore volume seems to have a constant value with variations lower than 5% at values higher than 40% of burn-off, which can be attributed to the experimental error in measurements or sample heterogeneity. Regarding to the micropore size distribution, n_{DA} values are smaller than 2, indicating a wide pore size distribution with a mean pore size diameter ranging from 1.4 to 1.8 nm.

Mercury intrusion and extrusion data are plotted in Figure 3.c, it can be observed that the longer the activation time, the higher the amount of mercury intruded in the sample, and therefore, the higher the porosity in the range of pores between 10 nm and 1000 nm. Pore size distribution calculated from mercury porosimetry data are shown in Figure 3.d. It can be observed that there is a characteristic pore size around 50nm for all the samples. Concerning the influence of the activation time, there is an initial increase of

pores of 50 nm joined to a slight decrease in pores around 35 nm in diameter. This effect is likely due to the reaction of the carbonised rubber partially converted, which is covering the entrance of these small pores. At longer activation times, it is observed that the activation led to a significant increase in the range of mesopores, between 7 and 35 nm, see Figure 3.d.

The SEM micrographs in the case of the tyre char and in the case of the samples A9002 and A90020 at several magnifications are exposed in Figure 4. Tyre char and sample A9002, can be described as composed of particles aggregations minor than 0.1 μm[16, 17] (Figures 4.a and 4.b), except in the case of the sample A90020. In this sample, after 20 hours of activation process, it can be observed that it has been reduced the number of spherical particles in the surface, showing a smooth inner structure.

It could be concluded that when the reaction starts, there is a double phenomenon in order to develop the porosity. First, narrow micropores are created and then, these narrow micropores grow to produce wider micropores or even mesopores. This second process is the most relevant in terms of porosity development.

Influence of temperature on porous texture. Figure 5 shows the influence of activation temperature on the textural properties of the samples. In Figure 5.a a higher production of surface area for the samples obtained at 850ºC is shown. However, samples obtained at 900 and 950ºC show similar values. This fact could be explained due to the above described slower reaction rate at 850ºC, which allows a deeper CO_2 diffusion inside the particle, and then, a higher microporosity surface development.

Pore volume distribution produced in different pore size ranges are plotted in Figures 5.b, 5.c and 5.d. It is observed that there is the same trend for total and micropore volumes than for surface area: the higher the activation, the higher the volume.

However, when data at different temperatures are compared, it can also be pointed out a slight variation for samples obtained at 850ºC with higher values for the same percentage of burn-off, confirming the increase in surface area detailed in the previous paragraph. However, a different trend can be seen in the case of the narrow microporosity, where a maximum has been achieved and no influence of reaction temperature has been observed, see Figure 5.d.

Temperature influence over textural properties during a physical activation process is not clear in the literature[15-17]. Merchant et al.[17] related the development of porosity with the reaction regime. Thus, activation reactions performed with chemical kinetic control, regime I[19], should produce the same properties into solids, no matter the reactor design or work conditions, as the CO_2 diffusion into the solid is favoured. The slight differences observed in the textural properties may be due to slight deviations in reaction conditions from those of the regime I.

Phenanthrene adsorption isotherm analysis. Phe adsorption isotherms for several samples with different grade of porosity, A9002, A90010, A90020, A90036, were obtained at 150ºC, see Figure 6. All the adsorption isotherms are close to type I. Therefore, the adsorption is mainly produced in the micropores with an average pore size twice the Phe molecular size (an estimated value of 0.7 nm was calculated using Materials Studio software).

In previous studies[12], it was demonstrated that there is a direct relationship between the Phe adsorption capacity of a certain activated carbon and its total micropore volume, as well as an influence of multilayer adsorption in pores others than micropores. In this way, as it was expected the higher the burn-off percentage, the higher their microporosity and the higher the adsorption capacity. During the activation reaction, not only changes in microporosity occurred, but they were also observed in all the different

ranges of pores (see Table 1). Therefore, it was proposed a relationship between the global parameter of burn-off and Phe adsorption capacity.

The experimental isotherms were fitted to the Langmuir, Freundlich and Dubinin Radushkevich adsorption models. In general, acceptable or good correlation coefficients were obtained for all the fittings. However, the Freundlich equation was chose to describe the experimental Phe adsorption isotherms, see Figure 6. Only this Model showed deviations lower than 5 % for the whole range of concentrations and all the samples when the experimental and predicted results were compared by residuals. .The Freundlich equation is commonly used in the form:

$$W = K_f \cdot C_0^{1/n_f} \qquad [3]$$

Where:

W is Phe adsorption capacity, mol Phe/kg adsorbent.

C_0 is the Phe concentration in the gas stream, mol Phe/m^3.

K_f and n_f are empirical constants characteristic of every adsorbate-adsorbent pair.

The Freundlich model is an empirical relationship based on the assumption of a logarithmic decrease in adsorption heat with adsorption surface coverage, therefore, allows for the averaging of different multilayer adsorption energies and different adsorption sites, which are both affected by the size and distribution of pores in an adsorbent[20]. Thus, the multilayer process involved in the Phe adsorption is taken into account.

A linear correlation was found between the burn-off and the K_f parameters (Table 2), with a correlation coefficient higher than 0.98. As K_f can be considered as an indicator of the adsorbent adsorption capacity , there is a linear correlation between the activation of tyre char and its Phe adsorption capacity. On the other hand, a maximum is observed

in the values obtained for n_f (Table 2), which denotes the adsorption strength[21]. Therefore, the activation process is not only producing a higher capacity to adsorb Phe, but it is also decreasing the strength of adsorption, which is interesting in order to regenerate the activated carbon.

Summarising, the textural properties of the activated carbons obtained from tyre char depend on the burn-off and they are independent of the conditions used to carry out the reaction as long as it is performed under kinetic regime I. In addition, the evolution of porosity can be described as a double phenomenon. In the fist step, narrow micropores are created once the reaction starts. Latter, a secondary step of the reaction supposed the destruction of narrow microporosity to generate wider pores. This porosity evolution in the activated carbons, as the reaction progresses, generates an increase in Phe adsorption capacity, as well as a decrease in the adsorption strength, which is an important factor in the desorption process during the activated carbon regeneration step.

Acknowledgements

This work has been partially supported by the General Council of Aragón, D.G.A., Spain (Pre-Doc. Grants of T. García and J.M. López) and the Spanish Science and Technology Ministry for the PPQ-4145 and the, R. Murillo and M.S. Callén, Ramón y Cajal Program.

Nomenclature

%Burn-off	Degree of carbon loss during activation
BET	Brunauer, Emmet and Teller
C_0	Phe inlet concentration, mol Phe/m^3

C_f	amount of fix carbon in char
$C_{Phe}(t)$	Phe concentration each time, mol Phe/m^3
DA	Dubinin-Astakov
DR	Dubinin Radushkevich
E_{DA}	adsorption energy
Kf	Characteristic Freundlich constant of this system
IUPAC	International Union of Pure and Applied Chemistry
L_{DA}	average pore width, nm
m_0	initial weigh of sample, kg.
$m_{0(mf)}$	initial weigh of sample moisture free, kg.
m_{CA}	weight of adsorbent, kg.
m_f	final weigh of solid, kg
n_{DA}	Pore size distribution parameter
nf	Characteristic Freundlich constant of this system
PAHs	Polycyclic Aromatic Hydrocarbons
Phe	Phenanthrene
Q	gas flow through the solid, m^3/s
S_{BET}	Surface area, m^2/g
SEM	Scanning Electron Microscopy
T	Temperature, K
t_t	total time, s.
V_T	Total pore volume, cm^3/g
W	amount of gas adsorbed per adsorbent mass unit at a determinate Phe concentration, mol/kg
W_{CO2}	Narrow micropore volume. cm^3/g
W_{exp}	adsorption capacity, mol Phe/kg adsorbent
W_{N2}	Total micropore volume, cm^3/g

Literature Cited

(1) Conesa J.A.; Font R.; Fullana A.; Caballero J.A. Kinetic model for the combustion of tyre wastes. *Fuel* **1998,** *77,* 1469-1475.

(2) Mastral, A.M.; Callen M.S.; Murillo R.; Garcia T. Combustion of high calorific value waste material: Organic atmospheric pollution. *Env. Sci. & Tech.* **1999,** *33,* 4155-4158.

(3) Mastral A.M., Murillo R., Callen M.S., Perez-Surio M.J., Mayoral M.C.. Assessment of the tyre role in coal-tyre hydroprocessing. *Energy and Fuels* **1997,** *11(3),* 676-680.

(4) Berrueco C., Esperanza E., Mastral F.J., Ceamanos J., García-Bacaicoa P., Pyrolysis of waste tyres in an atmospheric stacic-bed batch reactor: analysis of the gases obtained, *J. Anal. Appl. Pyrolysis*, **2005**, 65-73.

(5) Srinivasakannan C., Abu Bakar M.Z., Production of activated carbon from rubber wood sawdust, *Biomass & Bioenergy* **2004**, *27(1)*, 89-96.

(6) Williams P.T., Brindle A.J. Temperature selective condensation of tyre pyrolysis oils to maximise the recovery of single ring aromatic compounds. *Fuel* **2003**, *82,* 1023-1031.

(7) Cunliffe A.M., Williams P.T. Influence of Process Conditions on the Rate of Activation of Chars Derived from Pyrolysis of Used Tyres. *Energy and Fuels* **1999,** *13,* 166-175.

(8) Teng H., Serio M.A., Wojtowicz M.A., Baislakis R., Solomon P.R. Reprocessing of used tyres into activated carbon and other products. *Ind. Eng. Chem. Res.* **1995,** *34(9),* 3102-3111.

(9) Zabaniotou A.A., Stavropoulos G. Pyrolysis of used automobile tyres and residual char utilization. *J. Anal. Appl. pyrolysis* **2003,** *70,* 711-722.

(10) Mui E.L.K, Ko D.C.K., McKay G., Production of active carbons from waste tyres- a review, Carbon, **2004**, 42, 2789-2805.

(11) Raja S., Valsaraj K.T. Adsorption and Transport of Gas-Pahse Naphthalene on Micron-Size Fog Droplets in Air. *Environ. Sci. Technol.* **2004***, 38,* 763-768.

(12) Mastral A.M., Garcia T., Murillo R., Callen M.S., Lopez J.M., Navarro M.V. PAH mixture removal from hot gas by porous carbons. From model compounds to real conditions. *Ind. & Eng. Chem. Res.* **2003,** *42(21),* 5280-5286.

(13) Mastral A.M., Murillo R., Callen M.S., Garcia T. Application of coal conversion technology to tyre processing. *Fuel Proc. Tech.* **1999**, *60 (3)*, 231-242.

(14) Ariyadejwanich P., Tanthapanichakoon W., Nakagawa K., Mukai S.R., Tamon H. Preparation and characterization of mesoporous activated carbon from waste tyres, *Carbon* **2003**, *41*, 157-164.

(15) Cunliffe A.M., Williams P.T. Properties of chars and activated carbons derived from the pyrolysis of used tyres. *Env. Tech.* **1998,** *19*, 1177-1190.

(16) Helleur R., Popovic N., Ikura M. Characterization and potential applications of pyrolityc char from ablative pyrolysis of used tyres. *J. Anal. Appl. Pyrolysis* **2001,** *58*, 813-824.

(17) Ucar S., karagoz S, Ozkan A.R., Yanik J., Evaluation of two different scrap tires as hydrocarbon source by pyrolysis, Fuel, **2005**, in Press.

(18) Merchant A.A., Petrich M.A. Pyrolysis of scrap tyres and conversion of chars to activated carbon. *AIChE J* **1993,** *39(8),* 1370-1376.

(19) Szekely J., Evans J.W., Sohn H.Y. Academic Press. *Gas-Solid reactions, Cap. 4., New York,* 1976.

(20) Atkins P.W. Physical Chemistry, *3rd ed. New York: WH Freeman and Company*, 1986.

(21) Chang C.F., Chang C.Y., Holl W. Investigating the adsorption of 2-mercaptothiazoline on activated carbon from aqueous systems. *Journal of Colloid and Interface Science* **2004**, *272*, 52-58.

Table 1 Textural properties of products obtained from tyre char ($u=5\cdot10^{-3}$ m/s, 100%CO_2).

Ref.	S_{BET}, $\frac{m^2}{g}$	V_T, $\frac{cm^3}{g}$	W_{N2}, $\frac{cm^3}{g}$	W_{CO2}, $\frac{cm^3}{g}$	n_{DA}	E_{DA}, $\frac{J}{mol}$	L_{DA}, nm
CHAR	62	0.34	0.03	0.01	1.48	12124	2
A9002	68	0.32	0.03	0.01	1.72	17810	1.4
A9008	165	0.42	0.08	0.07	1.64	17560	1.4
A90010	208	0.44	0.10	0.07	1.39	13140	1.8
A90014	280	0.50	0.14	0.08	1.58	16596	1.5
A90016	349	0.50	0.17	0.09	1.60	16718	1.4
A90020	442	0.66	0.22	0.10	1.44	13249	1.8
A90024	472	0.76	0.23	0.09	1.45	14818	1.6
A90030	481	0.76	0.24	0.11	1.64	13550	1.8
A90036	528	1.03	0.26	0.09	1.47	14632	1.6

Table 2 Data obtained from experimental isotherms fitting with Freundlich models.

	A9002	**A90010**	**A90020**	**A90036**
Burn-off	7.0	19.7	43.9	68.4
K_f, $mol.kg^{-1}(m^3.mol^{-1})^{1/n}$	0.63	0.77	1.62	2.20
n_f	3.7	12.8	8.8	6.7
Residual error	<5%	<5%	<5%	<5%
r^2	0.983	0.956	0.986	0.989

CAPTION FOR FIGURES

FIGURE 1. Swept Fixed Bed Reactor.

FIGURE 2 Carbon burn-off for tyre char reaction in relation to activation time and temperature.

FIGURE 3. a) N_2 and b) CO_2 isotherms, c) Mercury analysis and d) Pore Size Distribution for samples obtained at 900ºC.

FIGURE 4 Evolution of solid surface with activation by SEM pictures.

FIGURE 5 Evolution of different textural properties with activation. Symbols for different temperatures are: 950ºC ▲, 900ºC ●, 850ºC ◆.

FIGURE 6 Phenanthrene adsorption experimental data and Freundlich fitting isotherms for selected samples: A9002 ◆, A90010 ▲, A90020 ■, A90036 ●.

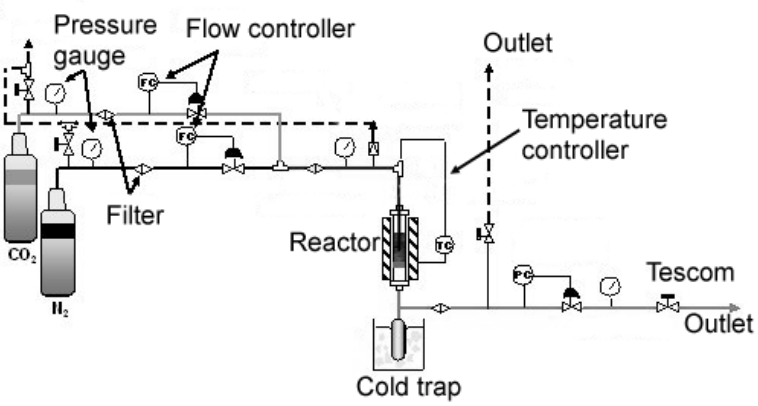
Pressure gauge
Flow controller
Outlet
Temperature controller
Filter
Reactor
Tescom
Outlet
Cold trap
CO2
H2

Figure 1.

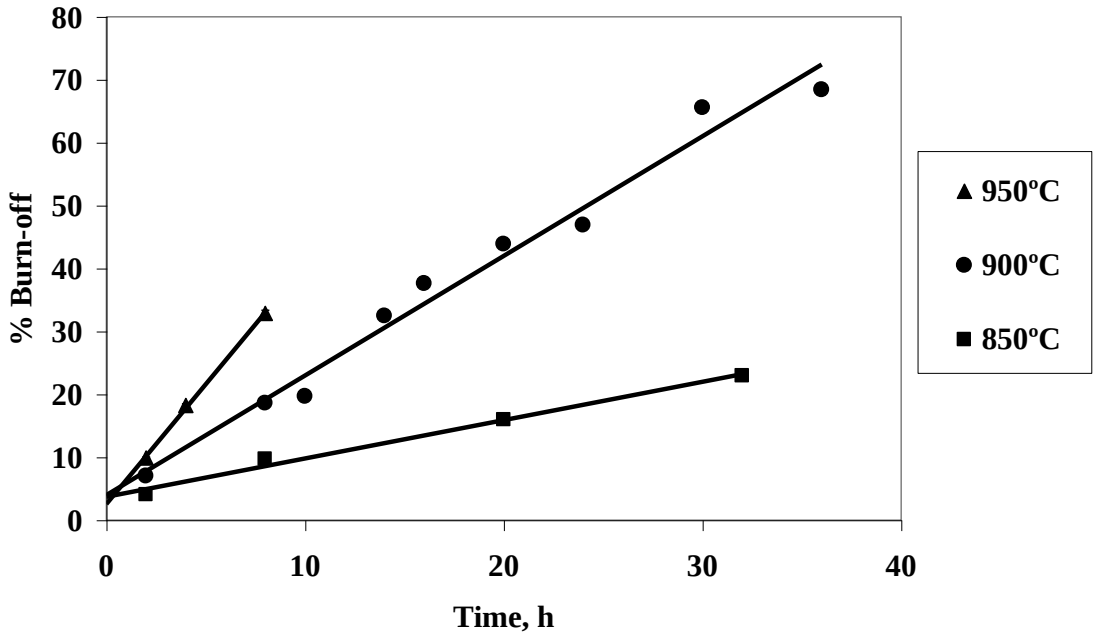
80
70
60
50
40
30
20
10
0
% Burn-off
0
10
20
30
40
Time, h
950ºC
900ºC
850ºC

Figure 2.

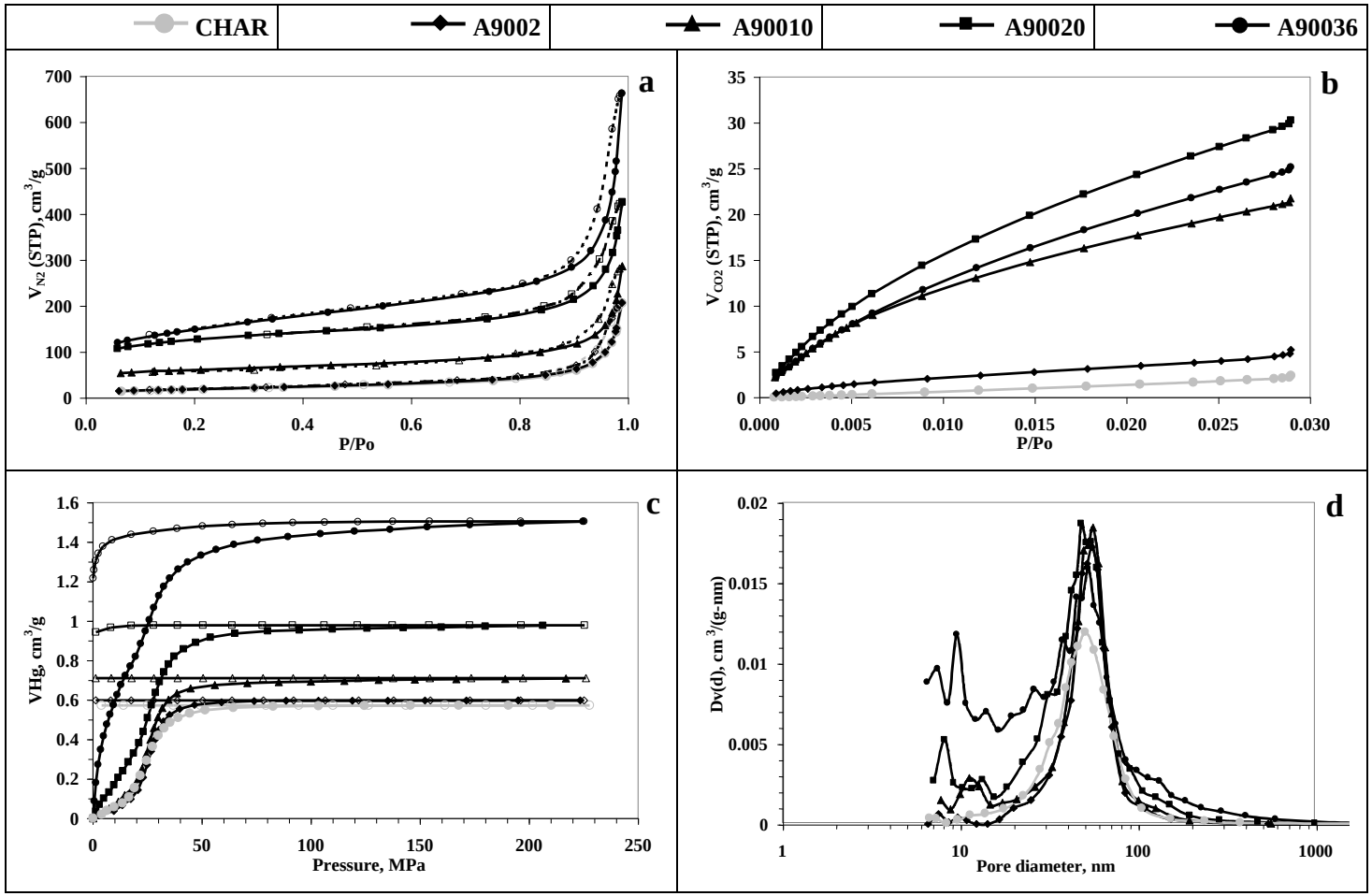
CHAR
A9002
A90010
A90020
A90036
a
b
c
d
V_{N2} (STP), cm^3/g
P/Po
V_{CO2} (STP), cm^3/g
P/Po
VHg, cm^3/g
Pressure, MPa
Dv(d), $cm^3/(g\cdot nm)$
Pore diameter, nm

Figure 3.

80 magnifications	3000 magnifications	25000 magnifications
		4.a) Tyre CHAR
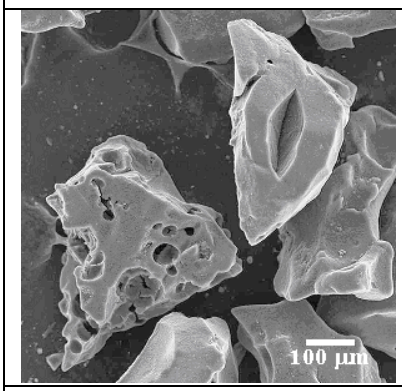	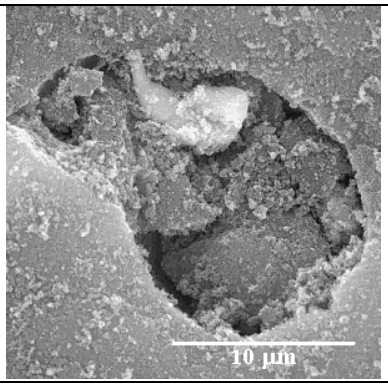	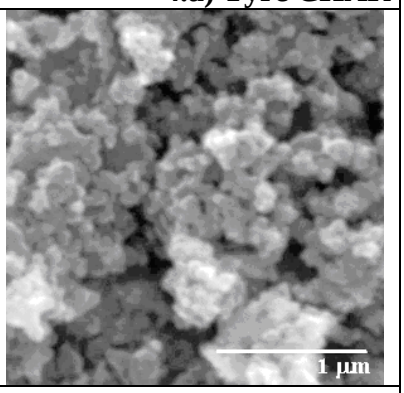
		4.b) A9002
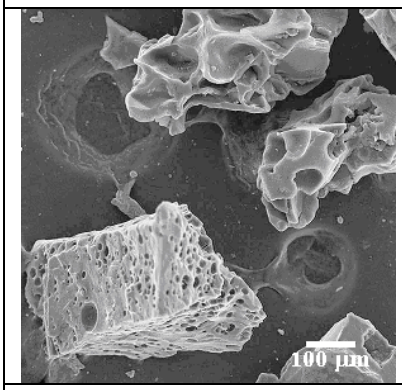	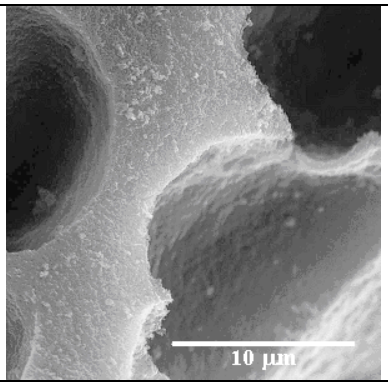	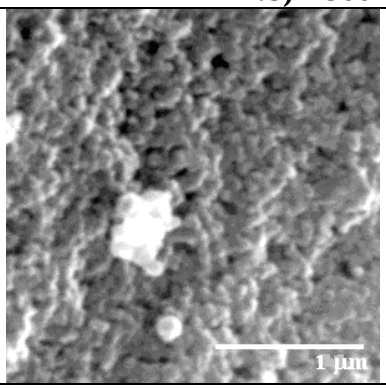
		4.c) A90020
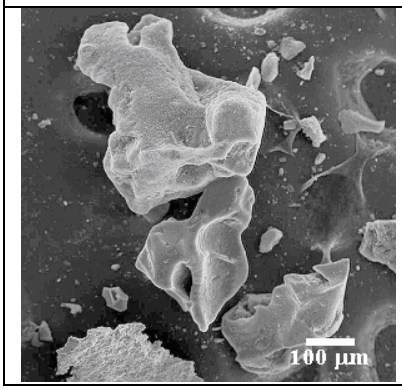	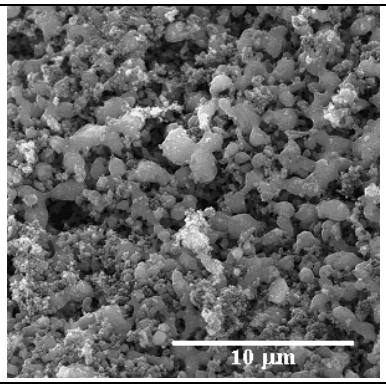	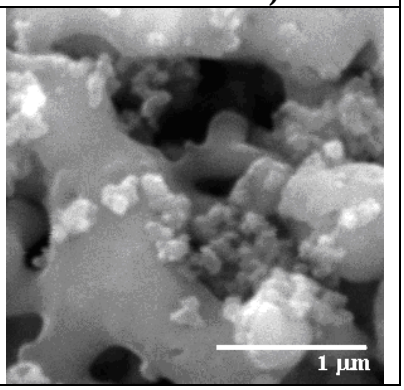

Figure 4.

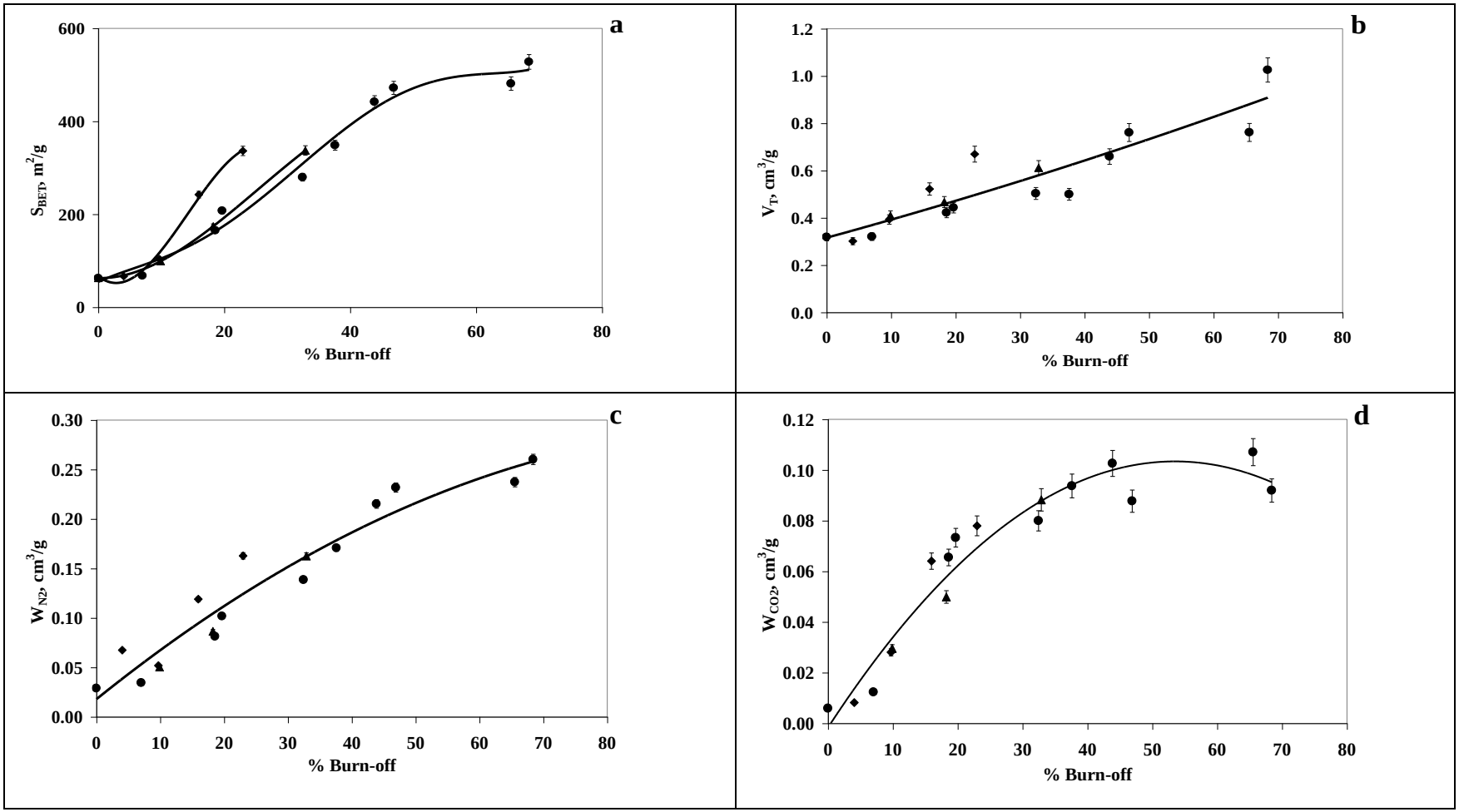
a
600
400
200
0
S_{BET}, m^2/g
0
20
40
60
80
% Burn-off
b
1.2
1.0
0.8
0.6
0.4
0.2
0.0
V_T, cm^3/g
0
10
20
30
40
50
60
70
80
% Burn-off
c
0.30
0.25
0.20
0.15
0.10
0.05
0.00
W_{N2}, cm^3/g
0
10
20
30
40
50
60
70
80
% Burn-off
d
0.12
0.10
0.08
0.06
0.04
0.02
0.00
W_{CO2}, cm^3/g
0
10
20
30
40
50
60
70
80
% Burn-off

Figure 5.

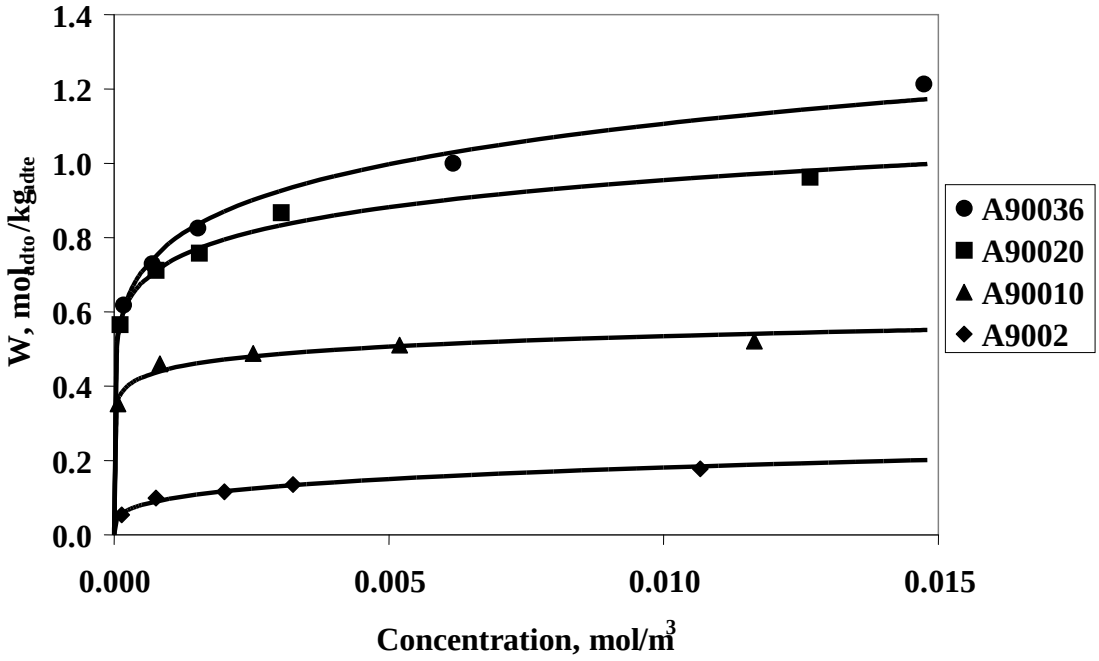
1.4
1.2
1.0
0.8
0.6
0.4
0.2
0.0
W, mol$_{adto}$/kg$_{adte}$
0.000
0.005
0.010
0.015
Concentration, mol/m^3
A90036
A90020
A90010
A9002

Figure 6.